

gap of our tin films. The behavior we have observed in these films in a perpendicular magnetic field was consistent with a study based on Tinkham's vortex model throughout the range from zero up to the critical field. This appears to be the most direct experimental evidence in support of the model presently available.

Note added in proof. Since this paper was submitted it has come to our attention that Maki [Ann. Phys. (N. Y.) **34**, 363 (1965)] has solved the G-L equations

for a film in a perpendicular field, showing that the vortex structure is indeed a stable solution for all values of κ in a sufficiently thin film.

ACKNOWLEDGMENTS

We would like to thank Vincent D. Arp, Richard H. Kropschot, Hans Meissner, Yoshiko Ohori, and George H. Wallace for valuable discussions and contributions to this work.

Nuclear Spin Relaxation in Molybdenum Metal*

ALBERT NARATH AND DONALD W. ALDERMAN†

Sandia Laboratory, Albuquerque, New Mexico

(Received 1 October 1965)

The ^{95}Mo and ^{97}Mo nuclear spin-spin and spin-lattice relaxation rates in molybdenum metal have been studied in the temperature range $1 \leq T \leq 4^\circ\text{K}$. The transverse relaxation process is found to have an exponential time dependence (corresponding to a Lorentzian line shape) with characteristic times $T_2(^{95}\text{Mo}) = 10 \pm 1$ msec and $T_2(^{97}\text{Mo}) = 14 \pm 1$ msec which are independent of temperature. At 4.0°K the longitudinal relaxation times are $T_1(^{95}\text{Mo}) = 8.9 \pm 0.2$ sec and $T_1(^{97}\text{Mo}) = 7.6 \pm 0.2$ sec. The ratio $T_1(^{95}\text{Mo})/T_1(^{97}\text{Mo}) = 1.17 \pm 0.03$ is larger than the square of the nuclear moment ratio, $(\mu^{97}/\mu^{95})^2 = 1.0424$. This anomaly is attributed to an electric quadrupole process due to d -band conduction electrons. This process contributes significantly to the relaxation rate of ^{97}Mo but not to that of ^{95}Mo because of the large difference in nuclear quadrupole moments ($Q^{97}/Q^{95} = 9.2$). The known moment ratios are used to partition the observed rates into nuclear magnetic dipole (R_μ) and nuclear electric quadrupole (R_Q) contributions. The resulting values of R_Q yield quadrupole moment estimates $Q^{95} = (0.12 \pm 0.03) \times 10^{-24}$ cm² and $Q^{97} = (1.1 \pm 0.2) \times 10^{-24}$ cm². An approximate separation of R_μ into contact, core-polarization, and orbital rates has been achieved. The principal contribution to the Knight shift and to the conduction-electron susceptibility is shown to arise from the orbital magnetization of the d band. The results of this study provide an upper-limit estimate of about 3 for the electron-phonon enhancement of the s -electron specific heat.

I. INTRODUCTION

THE nuclear magnetic resonance (NMR) technique has proved to be a useful tool for the study of electronic properties of transition metals. For example, measurements of Knight shifts in Rh,¹ Pd,² and Pt³ metals have led in each case to a partitioning of the magnetic susceptibility and electronic specific heat into s -spin, d -spin, and orbital contributions. Recently, the influence of the spin and orbital electronic magnetizations on nuclear spin-lattice relaxation rates has been analyzed within the framework of the tight-binding approximation.⁴⁻⁶ The individual relaxation rates were shown to be additive. Since the net Knight shift is generally due to a balance between positive contact, positive orbital, and negative core polarization processes,

the steady-state and relaxation measurements yield complementary results. Because of the current interest in transition metals we have undertaken a systematic study of nuclear spin relaxation rates in $4d$ and $5d$ transition metals.⁷

The bcc group VIa metals (Cr, Mo, W) provide a particularly interesting application for these techniques. In contrast to other d -band metals, the VIa metals exhibit a remarkably small density of states at the Fermi surface, as evidenced by an unusually small linear specific heat coefficient. The magnetic susceptibility, on the other hand, is much larger in each case than the spin susceptibility estimated from the specific heat.

In a previous study,⁸ the spin-lattice relaxation time T_1 of ^{183}W was measured in tungsten metal in the temperature range $1-4^\circ\text{K}$. A comparison of the rate $(T_1 T)^{-1} = 0.027$ (sec²K)⁻¹ with the Knight shift $K = +1.06\%$ established that about 80% of the conduction-electron susceptibility of tungsten is due to orbital paramagnetism of the d electrons. The present work is concerned with a similar investigation of ^{95}Mo and ^{97}Mo in molybdenum metal. In addition to the usual nuclear-

* This work was supported by the U. S. Atomic Energy Commission.

† Summer student at Sandia Laboratory; Present Address: Department of Physics, Cornell University, Ithaca, New York.

¹ J. A. Seitchik, V. Jaccarino, and J. H. Wernick, Phys. Rev. **138**, A148 (1965).

² J. A. Seitchik, A. C. Gossard, and V. Jaccarino, Phys. Rev. **136**, A1119 (1964).

³ A. M. Clogston, V. Jaccarino, and Y. Yafet, Phys. Rev. **134**, A650 (1964).

⁴ J. Korringa, Physica **16**, 601 (1950).

⁵ Y. Yafet and V. Jaccarino, Phys. Rev. **133**, A1630 (1964).

⁶ Y. Obata, J. Phys. Soc. Japan **18**, 1020 (1963).

⁷ For preliminary results, see A. T. Fromhold, Jr., and A. Narath, Bull. Am. Phys. Soc. **10**, 606 (1965).

⁸ A. Narath and A. T. Fromhold, Jr., Phys. Rev. **139**, A794 (1965).

magnetic-dipole relaxation mechanisms, spin-lattice relaxation due to d -electron interactions with the ^{97}Mo nuclear electric quadrupole moment has been detected. The ^{97}Mo nuclear quadrupole moment has been calculated from the measured rate. Estimates of the relative contributions of s and d states to the magnetic relaxation rate and Knight shift have been obtained. As in tungsten, the orbital magnetization is found to dominate the Knight shift and susceptibility. This result is in accord with the striking similarity between the electronic structures of these metals.⁹

Our experimental techniques are discussed in Sec. II. The results of our measurements are presented in Sec. III and discussed in Sec. IV. A summary of our results is given in Sec. V.

II. EXPERIMENTAL DETAILS

Measurements were carried out on two different powdered (325 mesh) specimens of molybdenum, both of which had nominal purities of 99.95+%. Spectrographic analyses of these samples revealed tungsten contents of 0.4%¹⁰ and 0.01%.¹¹ All other impurity levels were below 50 ppm. Despite the relatively high tungsten content of one of the molybdenum samples, the measurements gave identical results in both cases within the indicated uncertainty limits. This lack of sensitivity to tungsten contamination is not surprising in view of the nearly identical physical properties of molybdenum and tungsten.

Previous room-temperature Knight-shift measurements were extended to 4°K using a Varian induction spectrometer. The cw signal was detected near 3 Mc/sec in the dispersion mode. The sample was contained in the platinized tip of a narrow-tail glass He Dewar.

The relaxation rates were determined in the range 1–4°K by crossed-coil transient-induction techniques. The necessary rf excitation was provided by an incoherent pulsed oscillator, operating near 9 Mc/sec, which was coupled to the sample through a 90-Ω vacuum-jacketed coaxial transmission line. The timing sequence was provided by a combination of Tektronix 160 Series pulse generators and a Hewlett-Packard digital time-delay generator. Critical time intervals were measured with a digital counter.

The magnetic field for the transient experiments was produced by a compensated (0–60 kOe) superconducting solenoid.¹² The solenoid was usually operated in the persistent mode. Temperature control was achieved by regulated pumping on a separate, vacuum-jacketed He sample Dewar which was inserted in the bore of the magnet. Temperature measurements were based on the ^4He vapor pressure scale.

The rf receiver consisted of a narrow-band preamplifier (Arenberg PA-620) followed by a wide-band amplifier

(Arenberg WA-600). The video output, after passing through a low-pass filter, was recorded by means of a Tektronix RM-564 storage oscilloscope. In order to eliminate errors in the signal-amplitude measurements due to receiver nonlinearities, a comparison method was adopted, as shown schematically in Fig. 1. A stable rf signal generator was connected through a fixed attenuator to one side of a solid-state SPDT rf switch.¹³ The switch was inserted between the preamplifier and wide-band amplifier and was triggered in such a way that a transient calibration signal was injected immediately after the nuclear-spin signal. The signal generator level was adjusted for each data point to give approximately equal amplitudes for the nuclear-spin and calibration signals. The variable attenuator following the rf switch was used to maintain a maximum-size image on the screen of the storage oscilloscope. After measuring the relative amplitudes of the two signals, the determination of the absolute amplitudes was accomplished by measuring the signal generator level by means of a Tektronix RM-45 oscilloscope equipped with a type-Z differential comparator. The over-all receiver accuracy was better than $\pm 1\%$. In practice, however, the reproducibility of our measured relaxation times was only ± 2 –3% because of limited signal-to-noise ratios.

Because of rather short dephasing times (T_2^*) caused by inhomogeneous broadening of the nuclear resonance ($T_2^* \ll T_2$), most of our observations were based on spin-echo signals produced by two equal-width (~ 25 -μsec) rf pulses.¹⁴ Identical results were obtained with a $\pi/2, \pi$ sequence.

Spin-lattice relaxation times (T_1) were determined by measuring the recovery of the longitudinal nuclear magnetization following a saturating comb (of duration less than T_1) which was composed of approximately 40–80 narrow ($\sim \pi/2$) rf pulses. This technique has the significant advantage over other methods that a uniform initial Boltzmann distribution ($T = \infty$) is easily imposed on the system even in the presence of severe inhomogeneous broadening. The importance of a uni-

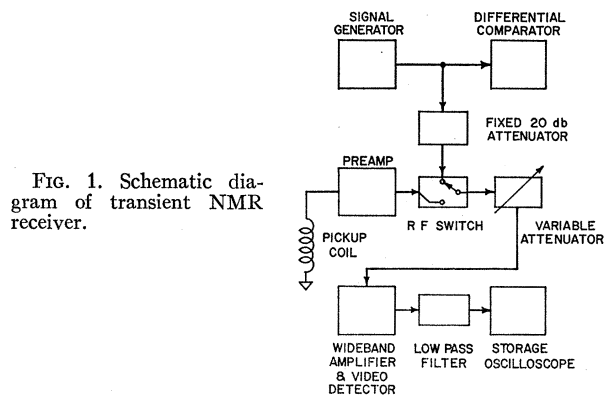


Fig. 1. Schematic diagram of transient NMR receiver.

⁹ T. L. Loucks, Phys. Rev. **139**, A1181 (1965).

¹⁰ Leytess Metal and Chemical Corp., 500 Fifth Avenue, New York 36, New York.

¹¹ United Mineral and Chemical Corp., 16 Hudson Street, New York 13, New York.

¹² Westinghouse Electric Corp., Pittsburgh, Pennsylvania.

¹³ Sanders Associates, Inc., Nashua, New Hampshire; Model DS11.

¹⁴ E. L. Hahn, Phys. Rev. **80**, 580 (1950).

form spin temperature for obtaining reliable T_1 's has been stressed by Simmons *et al.*¹⁵

Spin-spin relaxation times (T_2) were determined by measuring the echo amplitudes as a function of pulse separation in a two-pulse sequence. The interval between successive measurements was kept large compared to T_1 .

III. EXPERIMENTAL RESULTS

A. General Observations

The isotopes ^{95}Mo and ^{97}Mo occur in natural abundances of 15.8 and 9.6%, respectively. Both isotopes have spins of $\frac{5}{2}$.¹⁶ Nuclear resonance studies of aqueous K_2MoO_4 by Proctor and Yu¹⁷ have given $\mu^{95} = -(0.9098 \pm 0.0002)\mu_N$ and $\mu^{97} = -(0.9289 \pm 0.0002)\mu_N$. (These moments are uncorrected for diamagnetic shielding effects.) The magnetic moment ratio is¹⁷

$$\mu^{97}/\mu^{95} = 1.0210 \pm 0.0001. \quad (3.1)$$

The room-temperature Knight shift of molybdenum metal has been given by Aksenov¹⁸ as $+0.584 \pm 0.005\%$ relative to K_2MoO_4 . We have measured the Knight shift between 4 and 300°K. Our results are in excellent agreement with those of Aksenov and show that the shift is nearly temperature independent below 300°K. (At 4°K the field for resonance is 0.017% higher than at 300°K.)

Examples of typical ^{95}Mo and ^{97}Mo spin-echo signals obtained in the present work are shown in Fig. 2. In contrast to the "normal" shape of the ^{95}Mo echo, the ^{97}Mo signal is composed of two components of different widths. This shape is evidently the result of lattice-strain-induced first order quadrupole effects. The broad component appears to be due to the $\frac{1}{2} \leftrightarrow -\frac{1}{2}$ transition (which is not perturbed in this order), while the narrow component corresponds to the $\pm\frac{1}{2} \leftrightarrow \pm\frac{3}{2}$ and $\pm\frac{3}{2} \leftrightarrow \pm\frac{5}{2}$ transitions. This assignment is supported by the fact that the intensity ratio of the two components agrees very well with the predicted value of 9/26. The widths of the ^{95}Mo and the $\frac{1}{2} \leftrightarrow -\frac{1}{2}$ ^{97}Mo echoes are identical but have magnitudes which are only about one third of those expected from the magnetic field inhomogeneity. This observation suggests that these transitions are broadened by a slight spatial variation of the Knight shift. It is also noteworthy that the peak amplitudes of the ^{97}Mo and ^{95}Mo signals are in the ratio of their natural abundances, suggesting that the total nuclear magnetization was observed in our experiments. The above interpretation requires that $Q^{97}/Q^{95} \geq 4.6$, since no evidence of quadrupolar broadening was observed for the ^{95}Mo isotope. A large ratio of the two quadrupole moments has already been inferred by Proctor and Yu,¹⁷ as well as by Aksenov,¹⁸ on the basis of observed

¹⁵ W. W. Simmons, W. J. O'Sullivan, and W. A. Robinson, *Phys. Rev.* **127**, 1168 (1962).

¹⁶ J. Owen and I. M. Ward, *Phys. Rev.* **102**, 591 (1956).

¹⁷ W. G. Proctor and F. C. Yu, *Phys. Rev.* **81**, 20 (1951).

¹⁸ S. I. Aksenov, *Zh. Eksperim. i Teor. Fiz.* **35**, 300 (1958) [English transl.: *Soviet Phys.—JETP* **8**, 207 (1959)].

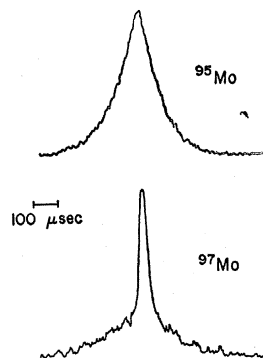


FIG. 2. Tracings of observed spin echoes following two equal-width rf pulses for ^{95}Mo and ^{97}Mo at 4.0°K in an external field of 32 kOe. The receiver gain for the ^{97}Mo signal was 6 db higher than for the ^{95}Mo signal.

cw linewidths. Kaufmann¹⁹ recently obtained a quantitative measure of this ratio by studying the linewidths in aqueous K_2MoO_4 whose viscosity was varied by the addition of sugar. Kaufmann obtained

$$Q^{97}/Q^{95} = 9.2 \pm 0.9. \quad (3.2)$$

Attempts to eliminate the strain broadening in our samples by high-vacuum annealing of the metal at 1200°C were only partially successful. Only a slight increase in the ^{97}Mo echo width could be achieved since prolonged annealing resulted in sintering of the powdered metal. Annealing had no detectable influence on the nuclear relaxation rates.

B. Spin-Spin Relaxation

The spin-spin relaxation rates were found to be independent of temperature in the range 1–4°K. The experimental decay curves are exponential as shown in Fig. 3. The measured relaxation times are

$$\begin{aligned} T_2(^{95}\text{Mo}) &= 10 \pm 1 \text{ msec}, \\ T_2(^{97}\text{Mo}) &= 14 \pm 1 \text{ msec}. \end{aligned} \quad (3.3)$$

An exponential decay of the transverse magnetization corresponds to a Lorentzian line shape in the frequency domain. The full-width at half intensity for such a line is given by $1/\pi T_2$, which yields 32 and 23 cps for ^{95}Mo and ^{97}Mo , respectively.

C. Spin-Lattice Relaxation

Measurements of T_1 at 4.0°K give

$$\begin{aligned} T_1(^{95}\text{Mo}) &= 8.9 \pm 0.2 \text{ sec}, \\ T_1(^{97}\text{Mo}) &= 7.6 \pm 0.2 \text{ sec}. \end{aligned} \quad (3.4)$$

The indicated uncertainty limits are rms deviations based on seven independent determinations for each isotope. A typical set of recovery curves is shown in Fig. 4. If the observed rates were due entirely to magnetic processes they would be in the ratio of the square of the respective nuclear magnetic dipole moments, $(\mu^{97}/\mu^{95})^2 = 1.0424$. Instead, the observed ratio is 1.17 ± 0.03 . In view of the large difference between the quadrupole moments of ^{95}Mo and ^{97}Mo it is reasonable to attribute this apparently anomalous ratio to contri-

¹⁹ J. Kaufmann, *Z. Physik* **182**, 217 (1964).

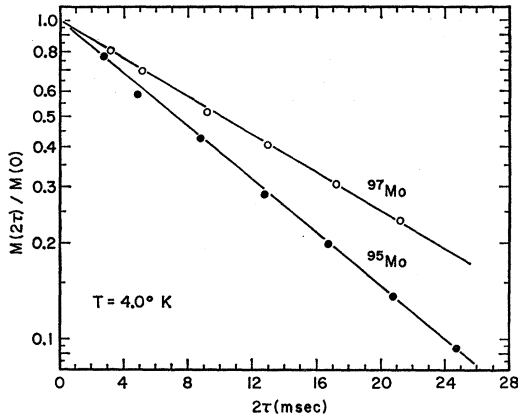


FIG. 3. Dependence of the spin-echo amplitudes for ^{95}Mo and ^{97}Mo on the time separation τ between the two rf pulses.

Contributions from an electric quadrupole relaxation process. Using $R_\mu \propto \mu^2$ and $R_Q \propto Q^2$ we obtain from (3.1), (3.2), and (3.4), in units of $(\text{sec}^\circ\text{K})^{-1}$

$$\begin{aligned} R_\mu^{95} &= 0.0281 \pm 0.0006, \\ R_\mu^{97} &= 0.0293 \pm 0.0006, \end{aligned} \quad (3.5)$$

and

$$\begin{aligned} R_Q^{95} &= 0.00004 \pm 0.00001, \\ R_Q^{97} &= 0.0036 \pm 0.0010, \end{aligned} \quad (3.6)$$

where R_μ and R_Q are the magnetic dipole and electric quadrupole rates ($R = 1/T_1T$), respectively.

The measured values of T_1T were found to be independent of temperature between 1 and 4°K.

IV. DISCUSSION

The observation of a narrow Lorentzian NMR in molybdenum is somewhat surprising. In fact, the mechanism which is responsible for this line shape is not understood at the present time. The effect of nuclear dipole-dipole interactions on the second moment $\langle \Delta\nu^2 \rangle$ of the NMR in a powder may be calculated for a primitive lattice from²⁰

$$\langle \Delta\nu_i^2 \rangle_{aa} = (\gamma_i/2\pi)^2 \left[(3f_i/5) (\gamma_i\hbar)^2 I_i(I_i+1) + (4f_j/15) (\gamma_j\hbar)^2 I_j(I_j+1) \right] \Sigma r^{-6}, \quad (4.1)$$

where f_i and f_j are the relative abundances of like and unlike isotopes, and γ_i and γ_j are their respective gyromagnetic ratios. Using a value of Σr^{-6} for the bcc lattice calculated by Gutowsky and McGarvey²¹ we obtain

$$\begin{aligned} (\langle \Delta\nu_{95}^2 \rangle_{aa})^{1/2} &= 91 \text{ cps}, \\ (\langle \Delta\nu_{97}^2 \rangle_{aa})^{1/2} &= 85 \text{ cps}. \end{aligned} \quad (4.2)$$

Dipolar broadening produces a nearly Gaussian line shape.²⁰ Defining an effective T_2 for such a shape as the

²⁰ See for example A. Abragam, *The Principles of Nuclear Magnetism* (Oxford University Press, London, England, 1961), Chap. IV.

²¹ H. S. Gutowsky and B. R. McGarvey, *J. Chem. Phys.* **20**, 1472 (1952).

time required for the magnetization to decay to $1/e$ of its initial value we find, using (4.2), $T_2(^{95}\text{Mo}) = 2.2$ msec and $T_2(^{97}\text{Mo}) = 2.4$ msec. These values are significantly shorter than the observed values (3.3), suggesting the presence of nondipolar spin-spin interactions which contribute strongly to the fourth moment. Indirect exchange coupling of like spins via the conduction electrons provides such a mechanism.^{22,23} The effect of indirect exchange on the transverse relaxation in molybdenum is difficult to treat quantitatively, however, because of the presence of two isotopes with non-zero magnetic moments. Additional complications arise from the low natural abundances of both species, and the lack of knowledge concerning the local variation of the strain-induced quadrupole interaction. It is conceivable, for example, that random quadrupole interactions might reduce significantly the number of like-neighbor spin pairs, and thus inhibit simultaneous spin-flip transitions. Since $Q^{97} > Q^{95}$, the resulting increase in the average phase-memory time (T_2) would be greater for ^{97}Mo than for ^{95}Mo , leading to $T_2(^{97}\text{Mo}) > T_2(^{95}\text{Mo})$ as observed. Furthermore, the exponential shape of the echo decay might be due to a superposition of Gaussian decays associated with a random spatial variation of dipolar spin-spin relaxation times.

The T^{-1} dependence of the measured spin-lattice relaxation times on temperature gives evidence that conduction electron mechanisms are responsible for both the magnetic dipole (3.5) and electric quadrupole (3.6) processes. In the following we make the usual assumption that the conduction bands are based on atomic s and d states.

The important contributions to the relaxation from magnetic interactions arise from (a) contact interactions

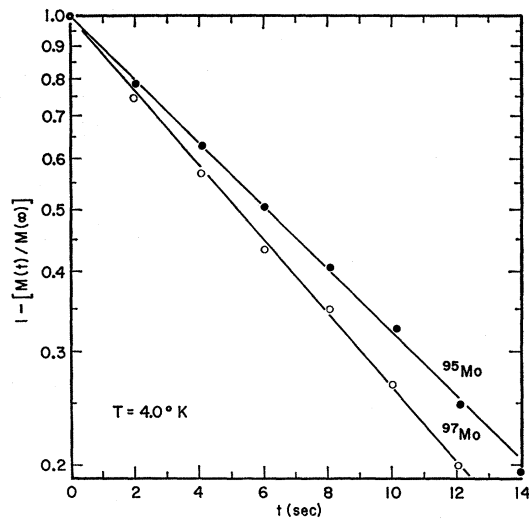


FIG. 4. Recovery of the ^{95}Mo and ^{97}Mo nuclear magnetizations after the application of a saturating comb.

²² M. A. Ruderman and C. Kittel, *Phys. Rev.* **96**, 99 (1954).

²³ N. Bloembergen and T. J. Rowland, *Phys. Rev.* **97**, 1679 (1955).

with the unfilled s band,⁴ (b) contact interactions with filled s shells which have been spin-polarized by exchange interactions with the unfilled d band,⁵ and (c) orbital interactions with the orbital moment of the d electrons.⁶ The respective relaxation rates are given in the tight-binding approximation by

$$\begin{aligned} (a) \quad R_s &= 2hk_B\gamma N^2 [H_{\text{hf}}(s)N_s(\zeta_0)]^2, \\ (b) \quad R_{\text{cp}} &= 2hk_B\gamma N^2 [H_{\text{hf}}(d)N_d(\zeta_0)]^2 \\ &\quad \times [\frac{1}{3}f^2 + \frac{1}{2}(1-f)^2], \quad (4.3) \\ (c) \quad R_{\text{orb}} &= 2hk_B\gamma N^2 [H_{\text{hf}}(\text{orb})N_d(\zeta_0)]^2 \\ &\quad \times [\frac{2}{3}f(2 - (5/3)f)], \end{aligned}$$

where h is Planck's constant, k_B is Boltzmann's constant, f is the average fractional admixture of $4d(\Gamma_6)$ states at the Fermi surface, and an electronic g value of two has been assumed. The $5s$ contact and $4d$ core-polarization hyperfine fields in the metal are given per electron by $H_{\text{hf}}(s)$ and $H_{\text{hf}}(d)$, respectively. The orbital hyperfine field per unit orbital angular momentum is given by $H_{\text{hf}}(\text{orb}) = 2\mu_B \langle r^{-3} \rangle$, where μ_B is the Bohr magneton and $\langle r^{-3} \rangle$ is an average over the radial distribution of d electrons near the Fermi surface. The state densities per unit energy interval at the Fermi energy ζ_0 for the s and d bands for one direction of the spin are denoted by $N_s(\zeta_0)$ and $N_d(\zeta_0)$, respectively.

We have estimated the magnitudes of the hyperfine fields in (4.3) in the following way. The $5s$ hyperfine field was calculated from the optical hfs data of Murakawa.²⁴ The ^{95}Mo hfs intervals of the $\lambda 5533$ $4d^5(^6S)5s^5S_2 \rightarrow 4d^5(^6S)5p^5P_2$ spectrum of Mo(I) yield $a(5s) = 0.072$ cm⁻¹, where $a(5s)$ is the magnetic hyperfine coupling constant of a single $5s$ electron. Using the known moment of ^{95}Mo we obtain a hyperfine field of 3.89×10^6 Oe, which we assume to be reduced in the metal by a factor of 0.7. The resulting field $H_{\text{hf}}(s) = 2.72 \times 10^6$ Oe compares with an estimate by Yafet and Jaccarino⁵ of 2.48×10^6 Oe for Nb (which has one less $4d$ electron than Mo) based on the term values of the Nb $4d^45s^1$ configuration. The core-polarization field was assumed to be given by $H_{\text{hf}}(d) = -0.1H_{\text{hf}}(s)$, which appears to be a reasonable approximation.²⁵ The orbital hyperfine field estimate, $H_{\text{hf}}(\text{orb}) = 0.30 \times 10^6$ Oe, was based on a Hartree-Fock free-atom value of $\langle r^{-3} \rangle = 3.2$ atomic units (a.u.),²⁶ which was adjusted by a factor of 0.75 to approximate its value in the metal.

With the exception of the admixture coefficient f , the only remaining unknowns in (4.3) are the s and d state densities. The total density of states, $N(\zeta_0) = N_s(\zeta_0) + N_d(\zeta_0)$, can be calculated from the recent specific heat measurements of Rorer *et al.*²⁷ ($\gamma = 1.85 \pm 0.05$ mJ/

²⁴ K. Murakawa, Phys. Rev. **100**, 1369 (1955); the spin assignments for ^{95}Mo and ^{97}Mo and hence the hyperfine coupling constants obtained in this paper are incorrect.

²⁵ See for example Ref. 1 (Rh), Ref. 2 (Pd), Ref. 3 (Pt), and Ref. 31 (Nb).

²⁶ A. J. Freeman and R. E. Watson, in *Magnetism* (Academic Press Inc., New York, 1965), Vol. IIA, Chap. IV.

²⁷ D. C. Rorer, D. G. Onn, and H. Meyer, Phys. Rev. **138**, A1661 (1965).

TABLE I. Summary of conduction-electron contributions to the ^{95}Mo and ^{185}W magnetic hyperfine fields, spin-lattice relaxation rates, and Knight shifts, in the respective metals, based on the fitting procedure described in the text. The values for tungsten are taken from Ref. 8 and are indicated by parentheses.

	H_{hf} (10^6 Oe)	R [10^{-2} (sec $^\circ\text{K})^{-1}$]		K (%)
		$f=1$	$f=\frac{2}{3}$	
Contact	+2.72 (+3.85)	1.56 (2.21)	1.36 (2.05)	+0.09 (+0.19)
Core	-0.27 (-0.38)	0.68 (0.20)	0.41 (0.12)	-0.11 (-0.10)
polarization				
Orbital	+0.30 (+0.56)	0.56 (0.29)	1.03 (0.53)	+0.59 (+0.97)
		$f=1$	$f=\frac{2}{3}$	
	$N_s(\zeta_0)$ (10^{11} cgs/atom)	=0.20 (0.26)	0.18 (0.25)	
	$N_d(\zeta_0)$ (10^{11} cgs/atom)	=2.25 (1.34)	2.27 (1.35)	

mole $^\circ\text{K}^2$), giving $N(\zeta_0) = 2.45 \times 10^{11}$ cgs/atom. The total relaxation rate, $R_\mu = R_s + R_{\text{cp}} + R_{\text{orb}}$, is a very sensitive function of the relative s and d densities at the Fermi surface. As in the case of tungsten,⁸ agreement between calculated and observed rates can be achieved by treating $N_s(\zeta_0)/N_d(\zeta_0)$ as an adjustable parameter. The resulting fit for two reasonable values of f , is compared in Table I with our previous results for tungsten. In both metals the largest contribution to R_μ results from the contact interaction, although in the case of molybdenum the core-polarization and orbital rates also appear to be important.

The Knight shift resulting from the above interactions is given by

$$\Delta H/H \equiv K = K_s + K_{\text{cp}} + K_{\text{orb}}, \quad (4.4)$$

with

$$\begin{aligned} K_s &= (\mu_B N)^{-1} H_{\text{hf}}(s) \chi_s, \\ K_{\text{cp}} &= (\mu_B N)^{-1} H_{\text{hf}}(d) \chi_d, \\ K_{\text{orb}} &= (\mu_B N)^{-1} H_{\text{hf}}(\text{orb}) \chi_{VV}, \end{aligned} \quad (4.5)$$

where N is Avogadro's number and χ_{VV} is the orbital magnetic susceptibility. The molar s - and d -spin susceptibilities are related to the corresponding state densities by

$$\begin{aligned} \chi_s &= 2N\mu_B^2 N_s(\zeta_0), \\ \chi_d &= 2N\mu_B^2 N_d(\zeta_0). \end{aligned} \quad (4.6)$$

Thus, it is possible to combine the measured 4 $^\circ\text{K}$ Knight shift, $K = 0.57\%$, with (4.4) and (4.5) to obtain an estimate for χ_{VV} . Taking $\chi_{VV} = 110 \times 10^{-6}$ emu/mole gives the fit shown in the last column of Table I.

TABLE II. Comparison between the calculated and observed magnetic susceptibilities of molybdenum and tungsten (Ref. 8) in units of 10^{-6} emu/mole.

	Mo	W
$\frac{2}{3}\chi_s$	1.3	1.8
χ_d	23.4	13.9
χ_{VV}	110	96
χ_{dia}	-20	-30
$\chi_{(\text{calc})}$	115	82
$\chi_{(\text{exp})}^a$	89	59

^a Reference 28.

The results of the above analysis may be checked by comparing the measured susceptibility²⁸ with that calculated from the expression

$$\chi_{\text{total}} = \frac{2}{3}\chi_s + \chi_d + \chi_{VV} + \chi_{\text{dia}}, \quad (4.7)$$

where χ_{dia} is the diamagnetic contribution from the ion cores. The susceptibility calculated in this way, using (4.6) and the above value of χ_{VV} , is listed in Table II together with our previous results for tungsten. (The values of χ_{dia} for Mo and W were derived from the susceptibilities of Ag and Au, respectively.) An inspection of Table II reveals that the conduction electron susceptibilities of both metals are dominated by χ_{VV} . For this reason, the difference between $\chi(\text{calc})$ and $\chi(\text{exp})$ can be attributed to an overestimate ($\sim 31\%$) of χ_{VV} for both molybdenum and tungsten. Such overestimates could easily have resulted from choosing too small a value for $\langle r^{-3} \rangle$. If this were indeed the case it would imply that the reduction of $\langle r^{-3} \rangle$ relative to the free atom value is much smaller than is generally assumed. It is also possible, however, to bring $\chi(\text{calc})$ and $\chi(\text{exp})$ into agreement by assuming a larger value of $N_s(\zeta_0)/N_d(\zeta_0)$ than was obtained from the fit of our spin-lattice relaxation data. In order to obtain agreement between calculated and observed relaxation rates it was necessary to choose a very small value of $N_s(\zeta_0)$. The required density $N_s(\zeta_0) \times 10^{-11} \approx 0.19$ corresponds to a number of free electrons n_s given by

$$n_s = (5.89 \times 10^{30}) V^{-2} N_s(\zeta_0)^3, \quad (4.8)$$

where V is the molar volume. Using $V = 9.41 \text{ cm}^3$ we obtain $n_s = 0.013$. The same calculation⁸ for tungsten gave $n_s = 0.03$. These numbers appear to be much too small when compared to the usual estimates of 0.2–1 for transition metals.²⁹ The effect of varying n_s is demonstrated in Table III, which gives the total magnetic spin-lattice relaxation rate based on the same hyperfine fields and total state density used previously. Also listed are values of χ_{VV} which give agreement with the observed Knight shift in each case. It is readily apparent that values of n_s near 1 lead to serious overestimates of R_μ as well as underestimates of χ_{VV} . Reasonable values of χ_{VV} are obtained, however, for $n_s \approx 0.2$. The corresponding s density leads to a value of R_μ which exceeds the experimental rate by a factor of 3.6. Very similar conclusions apply in the case of tungsten.

From the above arguments one may conclude that a consistent explanation of the Knight shift and susceptibility of molybdenum can be achieved by assuming larger values of either $\langle r^{-3} \rangle$ or $N_s(\zeta_0)$ (or both) than assumed in the calculation of R_μ (Table I). An increase in $N_s(\zeta_0)$ cannot be rejected despite the resulting

²⁸ C. J. Kriessman, Rev. Mod. Phys. **25**, 122 (1953).

²⁹ It should be noted that the exact meaning of n_s as given by (4.8) becomes somewhat unclear in the presence of s - d interactions near the Fermi level. Thus, it is likely that the anomalously small electronic specific heat observed in VIa metals is reflected in both s and d densities. We shall therefore view n_s only as an effective number of s electrons.

TABLE III. The dependence of the ⁹⁵Mo magnetic relaxation rate ($f = \frac{2}{3}$) and the orbital susceptibility on the assumed number of free s electrons in molybdenum metal.

n_s	R_μ ($10^{-2} \text{ sec}^{-1} \text{K}^{-1}$)	χ_{VV} (10^{-6} emu/mole)
0.2	10.2	80
0.4	15.3	67
0.6	19.9	58
0.8	23.9	51
1.0	27.1	46

overestimate of the thermal relaxation rate in view of the possible consequences of electron-phonon and electron-electron interactions.³⁰ These many-body effects are believed to enhance the electronic specific heat [and hence $N(\zeta_0)$] over the “bare” electron value. This increase, however, is not reflected in the nuclear relaxation rates, the latter being determined only by the “bare” electron density. Thus, relaxation rates calculated on the basis of the measured specific heat are expected to be too large. The magnitude of this effect, however, particularly in transition metals, is unknown. From our analysis it is possible to conclude that the s -electron specific heat in molybdenum may be enhanced by a factor which does not exceed 3. In this connection it is interesting to compare our results with those reported for Nb.^{5,31} In that case, an arbitrary choice of $n_s = 1$ gave a calculated R_μ which was about 2.5 times larger than the observed value. As in the case of molybdenum, the niobium result is sensitive to the assumed value of n_s , and therefore yields no definite conclusions concerning the possible magnitude of many-body effects.

We now turn our attention to the quadrupole relaxation rate R_Q . The effectiveness of an electric quadrupole mechanism involving conduction electrons has been investigated by Mitchell³² and Obata.³³ It has generally been concluded that this process is unimportant in comparison to the magnetic relaxation processes. In fact, to our knowledge, the present measurement constitutes the first unequivocal detection of this effect. Using our notation, Obata's tight-binding estimate for the quadrupole rate due to d -band electrons is given by

$$R_Q = 2\pi k_B h^{-1} (e^2 Q_{\text{eff}}/I)^2 [3(2I+3)/245(2I-1)] \times [N_d(\zeta_0) \langle r^{-3} \rangle]^2 [(5/3)f^2 - 2f + 2], \quad (4.9)$$

where Q_{eff} is the effective nuclear electric quadrupole moment, which may differ from the true moment Q because of antishielding effects.³⁴ In metals, these effects are probably quite small and we shall assume therefore that $Q_{\text{eff}} = Q$. The quantities which appear in (4.9), with the exception of Q_{eff} , have already been discussed in connection with the analysis of R_μ . It is possible, therefore, to use the measured rates (3.6) to calculate Q . We

³⁰ See Refs. 5 and 31 for references to the pertinent theoretical papers.

³¹ J. Butterworth, Proc. Phys. Soc. (London) **85**, 735 (1965).

³² A. H. Mitchell, J. Chem. Phys. **26**, 1714 (1957).

³³ Y. Obata, J. Phys. Soc. Japan **19**, 2348 (1964).

³⁴ R. Sternheimer, Phys. Rev. **84**, 244 (1951).

find

$$\begin{aligned} Q^{95} &= (0.12 \pm 0.03) \times 10^{-24} \text{ cm}^2, \\ Q^{97} &= (1.1 \pm 0.2) \times 10^{-24} \text{ cm}^2. \end{aligned} \quad (4.10)$$

This result is independent of f within the quoted error limits.

V. CONCLUSIONS

The results of the present NMR investigation of molybdenum metal are remarkably similar to those obtained in our previous study of tungsten. Both of these metals are distinguished by very small electronic specific heats. This is a characteristic property which is shared by all transition metals and alloys with electron/atom ratios near six. On the basis of a rigid-band model this behavior may be interpreted as a minimum in the density-of-states curve for $n \approx 6$. Since all of the conduction electron contributions to the nuclear spin-lattice relaxation depend explicitly on the magnitude of $N(\zeta_0)$, the observed relaxation times in molybdenum and tungsten are quite long. Furthermore, the spin-dependent contributions to the Knight shift are also expected to be small, since these depend (through the magnetic susceptibility) on the density of states. The orbital susceptibility, on the other hand, is determined primarily by the energy width of the d band and the relative number of occupied states, and is therefore not expected to be as strongly influenced by the small value of $N(\zeta_0)$ as the spin susceptibilities. Thus, the conclusion derived from our NMR experiments that the orbital

magnetization is the dominant contributor to the Knight shift and magnetic susceptibility in molybdenum and tungsten appears to be reasonable.

Because of uncertainties in the hyperfine-field estimates the analysis of the Knight shift and relaxation data did not provide any quantitative information concerning the magnitude of electron-phonon and electron-electron interactions in molybdenum. It may only be concluded that the s -electron specific heat is enhanced at most by a factor of about 3 by these many-body effects. This conclusion hinges, of course, on the reliability of the tight-binding approximation.

The detection of a quadrupolar spin-lattice relaxation process in molybdenum due to the conduction electrons was made possible by the existence of two isotopes with nearly identical nuclear magnetic moments but quite different electric quadrupole moments. This mechanism makes a significant contribution to the observed T_1 of ^{97}Mo because the ratio Q/μ is relatively large for this isotope. The molybdenum quadrupole moments obtained in the present work appear to represent the first quantitative estimates of Q^{95} and Q^{97} .

ACKNOWLEDGMENTS

The authors wish to express their gratitude to Dr. A. T. Fromhold, Jr. for several helpful discussions, to H. R. Farley and D. C. Barham for their assistance in some of the experiments, and to C. J. Howard for his help in the design and construction of the pulsed-rf oscillator.

Errata

Cerium Magnesium Nitrate Temperature Scale from Nuclear Orientation, R. B. FRANKEL, D. A. SHIRLEY, AND N. J. STONE [Phys. Rev. **140**, A1020 (1965)]. Table I on p. A1022 contains errors in the first 8 entries of each of the first two columns. The first eight rows should read:

$(H/T)_{\text{initial}}$ $kG^{\circ}K^{-1}$	$(S/R)_{\text{calc}}$	$1/T_s^*$	$(1/T)_{\text{DR}}$	$(1/T)_{\text{FSS}}$
0.8	0.692	20	20	20
1.6	0.688	40	40	40
2.5	0.682	60	60	60
3.3	0.673	80	80	80
4.2	0.661	100	100	100
5.0	0.647	120	120	120
5.9	0.631	140	140	140
6.8	0.611	160	160	160

We thank Dr. R. P. Hudson for calling our attention to the erroneous values. These errors were completely unrelated to the research reported in our paper, but arose from a computational mistake. These entries were given simply to indicate that our data for $T > 0.006^{\circ}\text{K}$ agree with the DR scale, although they do not stringently test it. None of our conclusions are altered.